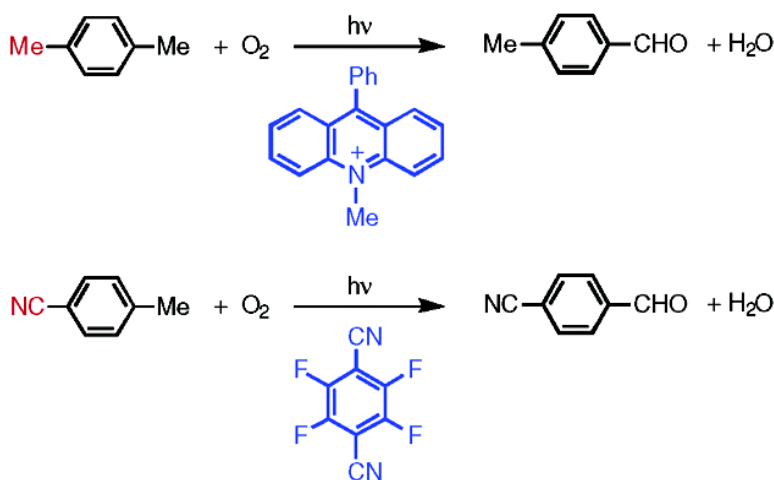


Selective Oxygenation of Ring-Substituted Toluenes with Electron-Donating and -Withdrawing Substituents by Molecular Oxygen via Photoinduced Electron Transfer

Kei Ohkubo, Kyou Suga, Kohei Morikawa, and Shunichi Fukuzumi

J. Am. Chem. Soc., **2003**, 125 (42), 12850-12859 • DOI: 10.1021/ja036645r • Publication Date (Web): 01 October 2003

Downloaded from <http://pubs.acs.org> on March 30, 2009



More About This Article

Additional resources and features associated with this article are available within the HTML version:

- Supporting Information
- Links to the 2 articles that cite this article, as of the time of this article download
- Access to high resolution figures
- Links to articles and content related to this article
- Copyright permission to reproduce figures and/or text from this article

[View the Full Text HTML](#)

Selective Oxygenation of Ring-Substituted Toluenes with Electron-Donating and -Withdrawing Substituents by Molecular Oxygen via Photoinduced Electron Transfer

Kei Ohkubo,[†] Kyou Suga,[†] Kohei Morikawa,[‡] and Shunichi Fukuzumi^{*†}

Contribution from the Department of Material and Life Science, Graduate School of Engineering, Osaka University, CREST, Japan Science and Technology Corporation, Suita, Osaka 565-0871, Japan, and Showa Denko, K. K., Kawasaki, Kanagawa 210-0867, Japan

Received June 12, 2003; E-mail: fukuzumi@ap.chem.eng.osaka-u.ac.jp.

Abstract: A ring-substituted toluene with an electron-withdrawing substituent, *p*-tolunitrile, is oxygenated by molecular oxygen to yield the corresponding aldehyde with tetrafluoro-*p*-dicyanobenzene as a photocatalyst under photoirradiation with an Hg lamp ($\lambda > 300$ nm). The oxygenation of a ring-substituted toluene with an electron-donating substituent, *p*-xylene, by molecular oxygen is also achieved with 10-methyl-9-phenylacridinium ion as a photocatalyst under visible light irradiation, yielding *p*-tolualdehyde exclusively as the final oxygenated product. Both the oxygenation reactions are initiated by photoinduced electron transfer from the ring-substituted toluene to the singlet excited state of the photocatalyst. The reason for the high selectivity in the photocatalytic oxygenation of various toluene derivatives by molecular oxygen is discussed on the basis of the photoinduced electron transfer mechanism that does not involve the autoxidation process (radical chain reactions). The reactive intermediates in the photocatalytic cycle are successfully detected as the transient absorption spectra and the electron spin resonance spectra.

Introduction

Molecular oxygen is an ideal reagent for economical and environmental benign oxygenation reactions because of its abundant availability and nontoxicity.^{1,2} Since direct concerted reactions between singlet molecules and triplet oxygen ($^3\text{O}_2$, $^3\Sigma_g^-$) are spin-forbidden, activation of oxygen by transition metal catalysts,³ photoexcitation to produce singlet oxygen ($^1\text{O}_2$),^{4,5} or generation of radical species that can react with $^3\text{O}_2$ directly (spin-allowed)⁶ is required to use molecular oxygen as a terminal oxidant. Among a variety of oxygenation reactions,

selective oxygenation of ring-substituted toluenes to aromatic aldehydes has merited special attention because of useful applications of aromatic aldehydes as key chemical intermediates for production of a variety of fine or specialty chemicals such as pharmaceutical drugs, dyestuffs, pesticides, and perfume compositions.⁷ A number of methods using inorganic oxidants such as chromium(IV),⁸ cobalt(III),⁹ manganese(III),¹⁰ cerium(IV),¹¹ benzeneseleninic anhydride,¹² or peroxydisulfate/copper ion¹³ have so far been reported for oxygenation of ring-substituted toluenes to aromatic aldehydes. However, their synthetic utility has been limited because of low yield and poor selectivity. Moreover, the use of stoichiometric amounts of inorganic oxidants should be avoided because of the environmental problem. *p*-Tolunitrile, which has an electron-withdrawing substituent (CN), is difficult to oxidize even by using inorganic oxidants to obtain *p*-cyanobenzaldehyde.¹⁴ *p*-Cyanobenzaldehyde has been synthesized industrially from *p*-

[†] Osaka University.

[‡] Showa Denko.

- (1) (a) Sheldon, R. A. *J. Chem. Technol. Biotechnol.* **1997**, *68*, 381. (b) Sheldon, R. A. *Chem. Ind. (London)* **1997**, 12. (c) *Oxygenases and Model Systems*; Funabiki, T., Ed.; Kluwer: Dordrecht, The Netherlands, 1997.
- (2) (a) Barton, D. H. R.; Martell, A. E.; Sawyer, D. T. *The Activation of Dioxygen and Homogeneous Catalytic Oxidation*; Plenum Press: New York, 1993. (b) Simandi, L. L. *Dioxygen Activation and Homogeneous Catalytic Oxidation*; Elsevier: Amsterdam, 1991.
- (3) (a) Mukaiyama, T. *Aldrich Acta* **1996**, *29*, 59. (b) Sheldon, R. A.; Arends, I. W. C. E.; Dijkstra, A. *Catal. Today* **2000**, *57*, 157. (c) Tsuji, J. *Synthesis* **1984**, 369. (d) Barton, D. H. R. *Tetrahedron* **1998**, *54*, 5805.
- (4) Foote, C. S.; Clennan, E. L. Properties and Reactions of Singlet Oxygen. In *Active Oxygen in Chemistry*; Foote, C. S., Valentine, J. S., Greenberg, A., Liebman, J. F., Eds.; Chapman and Hall: New York, 1995; pp 105–140.
- (5) (a) Bellus, D. *Adv. Photochem.* **1979**, *11*, 105. (b) Gorman, A. A. *Adv. Photochem.* **1992**, *17*, 217. (c) Lissi, E. A.; Encinas, M. V.; Lemp, E.; Rubio, M. A. *Chem. Rev.* **1993**, *93*, 699. (d) Adam, W.; Prein, M. *Acc. Chem. Res.* **1996**, *29*, 275.
- (6) (a) Ishii, Y.; Nakayama, K.; Takeno, M.; Sakaguchi, S.; Iwahama, T.; Nishiyama, Y. *J. Org. Chem.* **1995**, *60*, 3934. (b) Ishii, Y.; Iwahama, T.; Sakaguchi, S.; Nakayama, K.; Nishiyama, Y. *J. Org. Chem.* **1996**, *61*, 4520. (c) Yoshino, Y.; Hayashi, Y.; Iwahama, T.; Sakaguchi, S.; Ishii, Y. *J. Org. Chem.* **1997**, *62*, 6810. (d) Ishii, Y.; Sakaguchi, S.; Iwahama, T. *J. Synth. Org. Chem. Jpn.* **1999**, *57*, 24. (e) Tashiro, Y.; Iwahama, T.; Sakaguchi, S.; Ishii, Y. *Adv. Synth. Catal.* **2001**, *343*, 220. (f) Ishii, Y.; Sakaguchi, S.; Iwahara, T. *Adv. Synth. Catal.* **2001**, *343*, 393.
- (7) (a) Franz, G.; Sheldon, R. A. *Ullmann's Encyclopedia of Industrial Chemistry*, 5th ed.; VCH: Weinheim, Germany, 1991. (b) Sheldon, R. A.; Kochi, J. K. *Metal Catalyzed Oxidation of Organic Compounds*; Academic Press: New York, 1981; Chapter 10.
- (8) (a) Clarke, R.; Kuhn, A.; Okoh, E. *Chem. Br.* **1975**, *11*, 59. (b) Periasamy, M.; Bhatt, M. V. *Tetrahedron Lett.* **1978**, 4561.
- (9) Ballard, R. E.; McKillop, A. U.S. Patent 4 482 438, 1984.
- (10) Udupa, H. V. K. *Trans. Soc. Adv. Electrochem. Sci. Technol.* **1976**, *11*, 143.
- (11) (a) Baciocchi, E.; Giacco, T. D.; Rol, C.; Sebastiani, G. V. *Tetrahedron Lett.* **1985**, *26*, 3353. (b) Ho, T.-L. *Synthesis* **1973**, 347. (c) Syper, L. *Tetrahedron Lett.* **1966**, 4493.
- (12) Barton, D. H. R.; Hui, R. A. H. F.; Lester, D. J.; Ley, S. V. *Tetrahedron Lett.* **1979**, 3331.
- (13) Bhatt, M. V.; Perumal, P. T. *Tetrahedron Lett.* **1981**, *22*, 2605.
- (14) (a) Nicolaou, K. C.; Baran, P. S.; Zhong, Y.-L. *J. Am. Chem. Soc.* **2001**, *123*, 3183. (b) Nicolaou, K. C.; Montagnon, T.; Baran, P. S.; Zhong, Y.-L. *J. Am. Chem. Soc.* **2002**, *124*, 2245.

cyanobenzoyl chloride,¹⁵ *p*-cyanobenzyl halide,¹⁶ or dichloromethylbenzotrile.¹⁷

Radical species that can react with molecular oxygen can be readily generated by photoinduced electron-transfer reactions.^{18–20} The radical cations of ring-substituted toluenes readily deprotonate to give the corresponding benzyl radicals, which can react with oxygen directly to produce benzyl peroxy radicals, leading to the final oxygenated products.²¹ Rates of intermolecular photoinduced electron transfer reactions normally increase with increasing driving force of electron transfer (i.e., increasingly negative free energy change of electron transfer) to reach a diffusion-limited value.^{22–25} The free energy change of electron transfer is determined by the difference between the one-electron oxidation potentials of electron donors and the one-electron reduction potentials of electron acceptors. When the driving force of electron transfer is small, the rate is highly sensitive to minor changes in the driving force of electron transfer.^{22–25} For instance, only a 0.1 eV change in the driving force causes a 49 times difference in the electron-transfer rate.²⁶ Thus, the photoinduced electron transfer rates are finely controlled by choosing photocatalysts with different one-electron redox potentials. Since the one-electron oxidation potential of the oxygenated product is significantly more difficult (i.e., shifted to a more positive oxidation potential) than the reactant (electron donor), an appropriate choice of substrate and photocatalyst would enable selective oxygenation of the substrate via photoinduced electron transfer from the substrate electron donor to the excited state of the photocatalyst.

We report herein selective photoinduced oxygenation of ring-substituted toluenes with electron-donating or -withdrawing substituents by molecular oxygen that is achieved by choosing appropriate photocatalysts for efficient photoinduced electron transfer from ring-substituted toluenes to the excited state of sensitizers.²⁷ In contrast to oxidation by inorganic oxidants, no further oxidation of the initial oxygenated product occurs via photoinduced electron transfer to the sensitizer, leading to formation of the initial oxygenated product as the sole oxygenated product. The photoinduced electron-transfer mechanism of the photocatalytic oxygenation of ring-substituted toluenes is

well-clarified by the detection of reactive intermediates in the photocatalytic oxygenation reaction with use of laser flash photolysis and electron spin resonance (ESR) measurements as well as the analyses of the quantum yield determination.

Experimental Section

Materials. 1,4-Dicyanobenzene, 1,2,4,5-tetracyanobenzene, and halogenated dicyanobenzenes were purchased commercially. Toluene, *p*-, *m*-, and *o*-xylenes, 2,5-dimethoxytoluene, *p*-, *m*-, and *o*-tolualdehydes, *p*-tolunitrile, and *p*-tolualdehyde were also obtained commercially. 10-Methylacridinium iodide (AcrH⁺I⁻) was prepared by the reaction of acridine with methyl iodide in acetone, converted to the perchlorate salt (AcrH⁺ClO₄⁻) by the addition of magnesium perchlorate to AcrH⁺I⁻ in ethanol, and purified by recrystallization from methanol.^{28,29} Likewise, 1-methyl-3-cyanoquinolinium, 1-methylquinolinium, 1,4-dimethylquinolinium, and 1,2-dimethylquinolinium perchlorate salts were prepared by the reaction of the corresponding quinoline derivatives with methyl iodide in acetone, followed by the metathesis with Mg(ClO₄)₂.^{28,29} 10-Methyl-9-phenylacridinium perchlorate salt (AcrPh⁺ClO₄⁻) was prepared by the reaction of 10-methylacridone with the phenylmagnesium bromide in dichloromethane.³⁰ Potassium ferrioxalate used as an actinometer was prepared according to the literature and purified by recrystallization from hot water.³¹ Acetonitrile (MeCN), dichloromethane (CH₂Cl₂), and chloroform (CHCl₃) used as solvents were purified and dried by standard procedures.³² Deuterated [²H]₃acetonitrile (CD₃CN) and deuterated [²H]₁chloroform (CDCl₃) were obtained from Euri SO-TOP, CEA, France, and used as received.

Reaction Procedure. Typically, an MeCN solution (0.6 cm³) containing tetrafluoro-*p*-dicyanobenzene (1.0 × 10⁻² M) and *p*-tolunitrile (3.0 × 10⁻² M) in an NMR tube sealed with a rubber septum was saturated with oxygen by bubbling with oxygen through a stainless steel needle for 5 min. The solution was then irradiated with a mercury lamp through an acetophenone–methanol filter transmitting λ > 300 nm at room temperature. The irradiated solution was analyzed periodically by ¹H NMR spectroscopy. The ¹H NMR measurements were performed on a Japan Electron Optics JMN-AL300 (300 MHz) NMR spectrometer. The products of the photooxygenation of toluenes (3.0 × 10⁻² M) with AcrPh⁺ClO₄⁻ (1.0 × 10⁻² M) in oxygen-saturated CDCl₃ (0.6 cm³) were determined by ¹H NMR spectra. ¹H NMR (300 MHz, CDCl₃): *p*-tolualdehyde, δ 2.43 (s, 3H), 7.3–7.8 (m, 4H), 9.98 (s, 1H); *m*-tolualdehyde, δ 2.39 (s, 3H), 7.3–7.7 (m, 4H), 9.95 (s, 1H); *o*-tolualdehyde, δ 2.64 (s, 3H), 7.2–7.8 (m, 4H), 10.24 (s, 1H); benzaldehyde, δ 7.5–7.9 (m, 5H), 10.00 (s, 1H); isophthalaldehyde, δ 7.8–8.4 (m, 4H), 10.13 (s, 2H); phthalaldehyde, δ 7.8–8.0 (m, 4H), 10.53 (s, 2H). The product of the photooxygenation of *p*-tolunitrile (3.0 × 10⁻² M) with tetrafluoro-*p*-dicyanobenzene (1.0 × 10⁻² M) in oxygen-saturated CD₃CN (0.6 cm³) were determined by ¹H NMR spectra. ¹H NMR (300 MHz, CD₃CN): *p*-cyanobenzaldehyde, δ 7.8–8.1 (m, 4H), 10.05 (s, 1H); *p*-cyanobenzyl alcohol, δ 4.44 (s, 2H).

Quantum Yield Determination. A standard actinometer (potassium ferrioxalate)³¹ was used for the quantum yield determination of the AcrH⁺-photosensitized oxygenation of a ring-substituted toluene with oxygen. A square quartz cuvette (10 mm i.d.) that contained a CHCl₃ solution (3.0 cm³) of AcrH⁺ClO₄⁻ (1.0 × 10⁻⁴ M) and *p*-xylene [(5.0 × 10⁻²)–1.0 M] was irradiated with monochromatized light of λ = 358 nm from a Shimadzu RF-5300PC fluorescence spectrophotometer.

- (15) Rapoport, H.; Williams, A. R.; Lowe, O. G.; Spooncer, W. W. *J. Am. Chem. Soc.* **1953**, *75*, 1125.
 (16) (a) Hass, H. B.; Bender, M. L. *J. Am. Chem. Soc.* **1949**, *71*, 1767. (b) Wada, M.; Nakaoka, K. *Japan Patent* 60-166655, 1985.
 (17) Sugiyama, M.; Nakagawa, M.; Matsuzawa, M. *Japan Patent* 09-227490, 1997.
 (18) (a) Müller, F.; Mattay, J. *Chem. Rev.* **1993**, *93*, 99. (b) Mattay, J.; Martin, V. *Top. Curr. Chem.* **1991**, *159*, 219. (c) *Photoinduced Electron Transfer*; Fox, M. A., Chanon, M., Ed.; Elsevier: Amsterdam, 1988; Part C.
 (19) (a) Julliard, M.; Chanon, M. *Chem. Rev.* **1983**, *83*, 425. (b) Julliard, M.; Legris, C.; Chanon, M. *J. Photochem. Photobiol. A: Chem.* **1991**, *61*, 137. (c) Julliard, M.; Galadi, A.; Chanon, M. *J. Photochem. Photobiol. A: Chem.* **1990**, *54*, 79. (d) Lopez, L. *Top. Curr. Chem.* **1990**, *156*, 117. (e) Heumann, A.; Chanon, M. *Applied Homogeneous Catalysis with Organometallic Compounds*; Cornils, B., Herrmann, W. A., Ed.; VCH: Weinheim, Germany, 1996; pp 929–948.
 (20) Todd, W. P.; Dinnozenzo, J. P.; Farid, S.; Goodman, J. L.; Gould, I. R. *J. Am. Chem. Soc.* **1991**, *113*, 3601.
 (21) Fujita, M.; Ishida, A.; Takamuku, S.; Fukuzumi, S. *J. Am. Chem. Soc.* **1996**, *118*, 8566.
 (22) (a) Rehm, A.; Weller, A. *Ber. Bunsen-Ges. Phys. Chem.* **1969**, *73*, 834. (b) Rehm, A.; Weller, A. *Isr. J. Chem.* **1970**, *8*, 259.
 (23) Fukuzumi, S.; Ohkubo, K.; Suenobu, T.; Kato, K.; Fujitsuka, M.; Ito, O. *J. Am. Chem. Soc.* **2001**, *123*, 8459.
 (24) (a) Marcus, R. A. *Annu. Rev. Phys. Chem.* **1964**, *15*, 155. (b) Marcus, R. A. *Angew. Chem., Int. Ed. Engl.* **1993**, *32*, 1111.
 (25) Ebersson, L. *Electron-Transfer Reactions in Organic Chemistry*; Springer-Verlag: Berlin, 1987.
 (26) The value is obtained from 0.1/(2.3k_BT) = (1.602 × 10⁻¹⁹ J)/(2.3(1.381 × 10⁻²³ J K⁻¹)(298 K)) = 1.69; 10^{1.69} = 49.
 (27) A preliminary report has appeared: see Ohkubo, K.; Fukuzumi, S. *Org. Lett.* **2000**, *2*, 3647.

- (28) Roberts, R. M. G.; Ostović, D.; Kreevoy, M. M. *Faraday Discuss. Chem. Soc.* **1982**, *74*, 257.
 (29) Fukuzumi, S.; Koumitsu, S.; Hironaka, K.; Tanaka, T. *J. Am. Chem. Soc.* **1987**, *109*, 305.
 (30) Fukuzumi, S.; Ohkubo, K.; Tokuda, Y.; Suenobu, T. *J. Am. Chem. Soc.* **2000**, *122*, 4286.
 (31) Hatchard, C. G.; Parker, C. A. *Proc. R. Soc. London, Ser. A* **1956**, *235*, 518.
 (32) Perrin, D. D.; Armarego, W. L. F.; Perrin, D. R. *Purification of Laboratory Chemicals*, 4th ed.; Pergamon Press: Elmsford, NY, 1996.

Under the conditions of the actinometry experiments, both the actinometer and $\text{AcrH}^+\text{ClO}_4^-$ absorbed essentially all the incident light. The light intensity of monochromatized light of $\lambda = 358$ nm was determined as 2.78×10^{-8} einstein s^{-1} with a slit width of 20 nm. The photochemical reaction was monitored on a Shimadzu UV-3100PC spectrophotometer by using diluted the reaction solution. The quantum yields were determined from an increase in absorbance due to *p*-tolualdehyde ($\lambda = 290$ nm, $\epsilon = 1.4 \times 10^3$ $\text{M}^{-1} \text{cm}^{-1}$) and *p*-cyanobenzaldehyde ($\lambda = 309$ nm, $\epsilon = 2.7 \times 10^2$ $\text{M}^{-1} \text{cm}^{-1}$). To avoid the contribution by light absorption of the products, only the initial rates were used for determination of the quantum yields.

Fluorescence Quenching. Quenching experiments of the fluorescence of photocatalysts by ring-substituted toluenes were performed on a Shimadzu RF-5300PC fluorescence spectrophotometer. The monitoring wavelength was that corresponding to the maximum of the emission band of the photocatalyst. The solutions were deoxygenated by argon purging for 10 min prior to the measurements. Relative emission intensities were measured for MeCN or CHCl_3 solutions containing a photocatalyst (e.g., AcrPh^+ , 5.0×10^{-6} M) with electron donors at various concentrations (0 – 8.0×10^{-2} M). There was no change in the shape but there was a change in the intensity of the fluorescence spectrum by the addition of an electron donor. The Stern–Volmer relationship

$$I_0/I = 1 + K_{SV}[D] \quad (1)$$

was obtained for the ratio of the emission intensities in the absence and presence of ring-substituted toluenes (I_0/I) and the concentrations of quenchers [D]. The fluorescence lifetimes (τ) are 37 and 30 ns for AcrH^+ and 1.5 and 2.2 ns for AcrPh^+ in MeCN and CHCl_3 , respectively.^{21,23,33} The lifetimes in the presence of electron donors were determined by single photon counting on a Horiba NAES-1100 time-resolved spectrofluorophotometer. The fluorescence lifetimes of halogenated dicyanobenzenes were measured by a Photon Technology International GL-3300 with a Photon Technology International GL-302, nitrogen laser/pumped dye laser system, equipped with a four-channel digital delay/pulse generator (Stanford Research System Inc. DG535) and a motor driver (Photon Technology International MD-5020). The excitation wavelength was 337 nm. The observed quenching rate constants k_q ($= K_{SV}\tau^{-1}$) were obtained from the Stern–Volmer constants K_{SV} and the emission lifetimes τ .

Electrochemical Measurements. Cyclic voltammetry (CV) measurements were performed at 298 K on a BAS 100 W electrochemical analyzer in deaerated MeCN containing 0.1 M Bu_4NClO_4 (TBAP) as supporting electrolyte. A conventional three-electrode cell was used with a platinum working electrode (surface area of 0.3 mm^2) and a platinum wire as the counter electrode. The Pt working electrode (BAS) was routinely polished with a BAS polishing alumina suspension and rinsed with acetone before use. The second harmonic ac voltammetry (SHACV) measurements^{34,35} of toluene derivatives were performed on a BAS 100B electrochemical analyzer. The measured potentials were recorded with respect to the Ag/AgNO_3 (0.01 M) reference electrode. The redox potentials (vs Ag/AgNO_3) are converted to those vs SCE by adding 0.29 V.³⁶ All electrochemical measurements were carried out under an atmospheric pressure of argon.

Laser Flash Photolysis. The measurements of transient absorption spectra in the AcrPh^+ -photosensitized oxygenation of *p*-xylene with oxygen were performed according to the following procedures. The argon-, air-, or O_2 -saturated MeCN or CHCl_3 solution containing *p*-xylene (1.0×10^{-1} M) and AcrPh^+ (1.0×10^{-4} M) was excited by a Nd:YAG laser (Continuum, SLII-10, 4–6 ns fwhm) at $\lambda = 355$ nm with the power of 30 mJ/pulse. Photoinduced events were estimated by use of a continuous Xe lamp (150 W) and an InGaAs–PIN photodiode (Hamamatsu 2949) as a probe light and a detector, respectively. The output from the photodiodes and a photomultiplier tube was recorded with a digitizing oscilloscope (Tektronix, TDS3032, 300 MHz). The transient spectra were recorded for fresh solutions in each laser excitation. All experiments were performed at 298 K.

Electron-Transfer Reduction of AcrPh^+ . 10-Methyl-9-phenyl-acridinyl radical (AcrPh^*) in CHCl_3 or MeCN was prepared by the electron-transfer reduction of $\text{AcrPh}^+\text{ClO}_4^-$ (1.7×10^{-4} M) with tetramethylsemiquinone radical anion (0 – 1.7×10^{-4} M) generated by proportionation of tetramethyl-*p*-benzoquinone and tetramethylhydroquinone with tetrabutylammonium hydroxide.^{23,37}

ESR Measurements. An oxygen- or argon-saturated dichloromethane solution of AcrPh^+ (1.0×10^{-2} M) and *p*-xylene (5.0×10^{-1} M) was irradiated at 203 K with a high-pressure mercury lamp (USH-1005D) through a UV cutoff filter ($\lambda < 310$ nm) focused at the sample cell in the ESR cavity. The ESR spectra were taken on a Jeol JES-RE1XE and were recorded under nonsaturating microwave power conditions. The magnitude of the modulation was chosen to optimize the resolution and the signal-to-noise ratio (S/N) of the observed spectra. The g values were calibrated by use of an Mn^{2+} marker.

Results and Discussion

Photoinduced Electron-Transfer Reactivities of Photosensitizers. First, photoinduced electron-transfer reactivities of a variety of photosensitizers were examined with *p*-tolunitrile as an electron donor, which is difficult to oxidize because of the electron-withdrawing substituent (CN), to find an appropriate photosensitizer. The investigated photosensitizers are fluoro-, chloro-, and cyano-substituted benzenes, 1-methylquinolinium, and 10-methylacridinium ions as shown in Chart 1.

The redox and photophysical properties of the photosensitizers were determined by electrochemical and photophysical measurements (see Experimental Section), and data are summarized in Table 1.

Irradiation of the absorption band of the photosensitizers results in fluorescence in MeCN. The fluorescence of the photosensitizers was quenched by *p*-tolunitrile, and the quenching rate constants (k_q) were determined from the slopes of the Stern–Volmer plots and lifetimes of the singlet excited state of the photosensitizers (typical data are shown in Supporting Information, Figure S1). The k_q values thus obtained are also summarized in Table 1.

The free energy change of photoinduced electron transfer from *p*-tolunitrile to the singlet excited states of photosensitizers (ΔG_{et}^0 in electronvolts) is given by³⁸

$$\Delta G_{\text{et}}^0 = e(E_{\text{ox}}^0 - E_{\text{red}}^{0*}) \quad (2)$$

where e is elementary charge and E_{ox}^0 and E_{red}^{0*} are the one-electron oxidation potential of *p*-tolunitrile and the one-electron

(33) van Willigen, H.; Jones, G., II; Farahat, M. S. *J. Phys. Chem.* **1996**, *100*, 3312.

(34) Bard, A. J.; Faulkner, L. R. *Electrochemical Methods, Fundamental and Applications*; John Wiley & Sons: New York, 2001; Chapt. 10, pp 368–416.

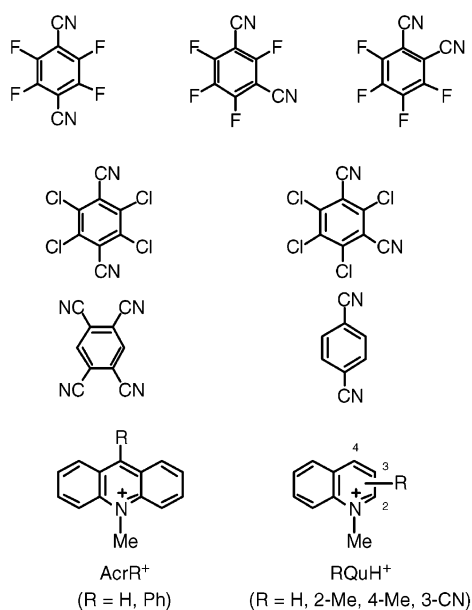
(35) The SHACV method provides a superior approach to directly evaluating the one-electron redox potentials in the presence of a follow-up chemical reaction, relative to the better-known dc and fundamental harmonic ac methods: (a) Bond, A. M.; Smith, D. E. *Anal. Chem.* **1974**, *46*, 1946. (b) Arnett, E. M.; Amarnath, K.; Harvey, N. G.; Cheng, J.-P. *J. Am. Chem. Soc.* **1990**, *112*, 344.

(36) Mann, C. K.; Barnes, K. K. *Electrochemical Reactions in Nonaqueous Systems*; Marcel Dekker: New York, 1970.

(37) (a) Fukuzumi, S.; Nakanishi, I.; Maruta, J.; Yorise, T.; Suenobu, T.; Itoh, S.; Arakawa, R.; Kadish, K. M. *J. Am. Chem. Soc.* **1998**, *120*, 6673. (b) Fukuzumi, S.; Nakanishi, I.; Suenobu, T.; Kadish, K. M. *J. Am. Chem. Soc.* **1999**, *121*, 3468.

(38) Kavarnos, G. J. *Fundamentals of Photoinduced Electron Transfer*; Wiley-VCH: New York, 1993.

Chart 1



reduction potential of the singlet excited state of photosensitizers, respectively.^{39,40}

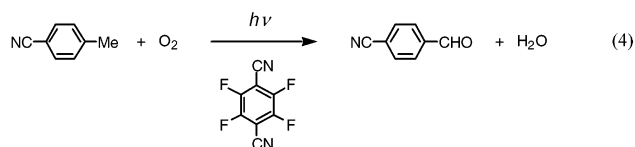
Figure 1 shows a plot of $\log k_q$ vs E_{red}^0 in MeCN, which exhibits a typical feature of an electron-transfer process: the $\log k_q$ value increases with an increase in E_{red}^0 , which corresponds to a decrease in ΔG_{et}^0 in eq 2, to reach a plateau value corresponding to the diffusion rate constant in MeCN ($2.0 \times 10^{10} \text{ M}^{-1} \text{ s}^{-1}$) as the photoinduced electron transfer becomes energetically more favorable (i.e., more exergonic).^{22,38} The dependence of k_q on ΔG_{et}^0 for adiabatic outer-sphere electron transfer has well been established by Marcus as given by

$$\frac{1}{k_q} = \frac{1}{k_{\text{diff}}} + \frac{1}{Z \exp[-(\lambda/4)(1 + \Delta G_{\text{et}}^0/\lambda)^2/k_B T]} \quad (3)$$

where k_{diff} is the diffusion rate constant, taken as $2.0 \times 10^{10} \text{ M}^{-1} \text{ s}^{-1}$ in MeCN; Z is the collision frequency, taken as $1 \times 10^{11} \text{ M}^{-1} \text{ s}^{-1}$; λ is the reorganization energy of electron transfer; and k_B is the Boltzmann constant.^{24,38} The solid line in Figure 1 calculated from eqs 2 and 3 with the λ value of 0.33 eV and E_{ox}^0 value of 2.64 V agrees with the experimental k_q values.⁴¹ Thus, the fluorescence quenching of photosensitizers by *p*-tolunitrile occurs via electron transfer from the *p*-tolunitrile to the singlet excited states of photosensitizers.

Photocatalytic Oxygenation of *p*-Tolunitrile with Oxygen by Use of Tetrafluoro-*p*-dicyanobenzene. Tetrafluoro-*p*-dicyanobenzene was chosen as a photocatalyst for oxygenation of *p*-tolunitrile with molecular oxygen, since the photoinduced electron transfer from *p*-tolunitrile to the singlet excited state of tetrafluoro-*p*-dicyanobenzene occurs efficiently (Table 2). Photoirradiation of the absorption band of tetrafluoro-*p*-dicyanobenzene ($\lambda_{\text{max}} = 312 \text{ nm}$) in oxygen-saturated acetonitrile

containing *p*-tolunitrile (30 mM) with an Hg lamp results in formation of *p*-cyanobenzaldehyde accompanied by disappearance of *p*-tolunitrile (eq 4). The product yield increase with



photoirradiation time is shown in Table 2.^{42,43}

The quantum yields (Φ) of the tetrafluoro-*p*-dicyanobenzene-photocatalyzed oxygenation of *p*-tolunitrile with O_2 were determined from the product formation rate under irradiation of monochromatized light of $\lambda = 312 \text{ nm}$ (see Experimental Section). The same Φ values are obtained for the photooxygenation reaction at different concentrations of O_2 (Figure 2a). The Φ values increase with an increase in concentration of *p*-tolunitrile [D] to approach a limiting value (Φ_{∞}) in accordance with eq 5

$$\Phi = \Phi_{\infty} K_{\text{obs}} [D] / (1 + K_{\text{obs}} [D]) \quad (5)$$

as shown in Figure 2a. Equation 5 is rewritten as eq 6

$$\Phi^{-1} = \Phi_{\infty}^{-1} [1 + (K_{\text{obs}} [D])^{-1}] \quad (6)$$

and the linear plots of Φ^{-1} versus $[D]^{-1}$ is shown in Figure 2b. The Φ_{∞} and K_{obs} values are obtained from the slope and intercept in Figure 2b as 0.47 and 14 M^{-1} , respectively. The K_{obs} value can be converted to the corresponding rate constant (k_{obs}) provided that the excited state of tetrafluoro-*p*-dicyanobenzene involved in the photocatalytic reaction is a singlet ($k_{\text{obs}} = K_{\text{obs}} \tau^{-1}$, $\tau = 3.2 \text{ ns}$). The k_{obs} value ($4.6 \times 10^9 \text{ M}^{-1} \text{ s}^{-1}$) agrees well with the corresponding k_q value determined independently by the fluorescence quenching ($4.9 \times 10^9 \text{ M}^{-1} \text{ s}^{-1}$; Supporting Information, Figure S1). Such agreement strongly indicates that the photocatalytic reaction proceeds via photoinduced electron transfer from *p*-tolunitrile to the singlet excited state of tetrafluoro-*p*-dicyanobenzene as shown in Scheme 1.

Electron transfer occurs from *p*-tolunitrile to the singlet excited state of tetrafluoro-*p*-dicyanobenzene (k_{et}) to give the radical ion pair. Deprotonation of *p*-tolunitrile radical cation (RH^+) occurs in competition with the back electron transfer from tetrafluoro-*p*-dicyanobenzene radical anion to *p*-tolunitrile radical cation. Benzyl radical (R^{\bullet}), which is the deprotonation product of *p*-tolunitrile radical cation, reacts with molecular oxygen to give the peroxy radical (Scheme 1). Protonation of the peroxy radical occurs to give the hydroperoxide, which decomposes to *p*-cyanobenzaldehyde.

According to Scheme 1, the quantum yield Φ is given as a function of concentrations of *p*-tolunitrile [D] by

$$\Phi = k_d k_{\text{et}} \tau [D] / (k_d + k_{\text{bet}}) (1 + k_{\text{et}} \tau [D]) \quad (7)$$

which agrees with the experimental observation (eq 5). The Φ value is independent of concentrations of O_2 , since the limiting

(39) Fukuzumi, S.; Tanaka, T. In *Photoinduced Electron Transfer*; Fox, M. A., Chanon, M., Eds.; Elsevier: Amsterdam, 1988; Part C, p 578.

(40) (a) Fukuzumi, S.; Kitano, T. *J. Chem. Soc., Perkin Trans. 2* **1991**, 41. (b) Fukuzumi, S.; Noura, S. *J. Chem. Soc., Chem. Commun.* **1994**, 287. (c) Fukuzumi, S.; Fujita, M.; Noura, S.; Ohkubo, K.; Suenobu, T.; Araki, Y.; Ito, O. *J. Phys. Chem. A* **2001**, *105*, 1857.

(41) The E_{ox}^0 value of *p*-tolunitrile in MeCN could not be determined directly by the electrochemical measurement because of the high oxidation potential and the irreversible oxidation.

(42) At prolonged reaction times, *p*-cyanobenzyl alcohol is also produced, probably due to the autooxidation process.

(43) In the case of 1,4-dicyanobenzene, photooxygenation of *p*-tolunitrile hardly occurred under the same experimental conditions as employed for the case of tetrafluoro-*p*-dicyanobenzene used as a photocatalyst. This is consistent with the much smaller k_q value of 1,4-dicyanobenzene than that of tetrafluoro-*p*-dicyanobenzene (Table 1).

Table 1. One-Electron Reduction Potentials, Fluorescence Lifetimes, Singlet Excited Energies, and Quenching Rate Constants in MeCN

	photosensitizer	E_{red}^0 (V) vs SCE	E_{red}^{0*} (V) vs SCE	τ^c (ns)	$E_{00}(S)^d$ (eV)	k_q^e ($M^{-1} s^{-1}$)
1	1,2,4,5-tetracyanobenzene	-0.74	3.17	4.3	3.81	1.5×10^{10}
2	1-methyl-3-cyanoquinolinium ion	-0.60 ^f	2.72 ^f	45 ^f	3.32 ^f	7.3×10^9
3	tetrafluoro- <i>p</i> -dicyanobenzene	-1.10	2.66	3.2	3.76	4.9×10^9
4	tetrafluoro- <i>o</i> -dicyanobenzene	-1.62	2.66	2.6	4.18	3.4×10^9
5	tetrafluoro- <i>m</i> -dicyanobenzene	-1.33	2.61	3.9	3.99	3.3×10^9
6	1,4-dicyanobenzene	-1.46	2.55	9.7	4.01	7.4×10^8
7	1-methylquinolinium ion	-0.96 ^f	2.54 ^f	20 ^f	3.50 ^f	2.2×10^8
8	1,4-dimethylquinolinium ion	-1.07 ^f	2.51 ^f	19 ^f	3.58 ^f	1.2×10^8
9	1,2-dimethylquinolinium ion	-1.05 ^f	2.46 ^f	15 ^f	3.51 ^f	8.7×10^7
10	10-methylacridinium ion	-0.43 ^g	2.32 ^g	37 ^g	2.75 ^g	<i>h</i>
11	tetrachloro- <i>p</i> -dicyanobenzene	-0.95	2.55	0.25	3.50	<i>i</i>
12	tetrachloro- <i>m</i> -dicyanobenzene	<i>j</i>		0.20	3.71	<i>i</i>

^a One-electron reduction potential of ground state. ^b One-electron reduction potential of singlet excited state. ^c Fluorescence lifetime of dicyanobenzene derivatives. ^d Singlet excited energy of dicyanobenzene derivatives. ^e Quenching rate constants of the photoinduced electron transfer from *p*-tolunitrile to photosensitizer in MeCN. ^f Taken from ref 40. ^g Taken from ref 23. ^h Too slow to be determined accurately. ⁱ No quench. ^j Irreversible CV wave.

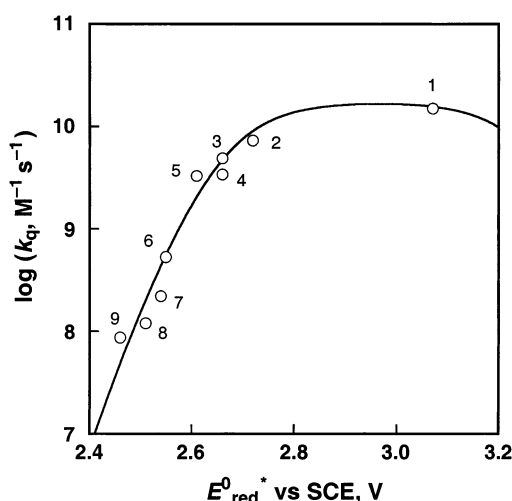
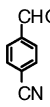
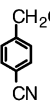


Figure 1. Plots of $\log k_q$ vs E_{red}^0 for the fluorescence quenching of various photosensitizers by *p*-tolunitrile in deaerated MeCN at 298 K. The curves represent the best fit to eqs 2 and 3; $E_{\text{ox}}^0 = 2.64$ V vs SCE and $\lambda = 7.6$ kcal mol⁻¹. Numbers refer to photosensitizers in Table 1.

Table 2. Reactant Conversion and Product Yields in Photooxygenation of *p*-Tolunitrile (3.0×10^{-2} M), Catalyzed by Tetrafluoro-*p*-Dicyanobenzene (1.0×10^{-2} M) in O₂-Saturated MeCN

time, h	conversion, %	yield, %	
			
0	0	0	0
1	6	6	0
2	9	9	1
4	18	15	3
8	27	22	4

quantum yield Φ_{∞} is determined by competition between the deprotonation of the radical cation (k_d) and the back electron transfer (k_{bet}): $\Phi_{\infty} = k_d / (k_d + k_{\text{bet}})$. It should be noted that no radical chain process (autoxidation) is involved in Scheme 1.

Selective Photocatalytic Oxygenation of *p*-Xylene with Oxygen by Use of 10-Methyl-9-phenylacridinium Perchlorate

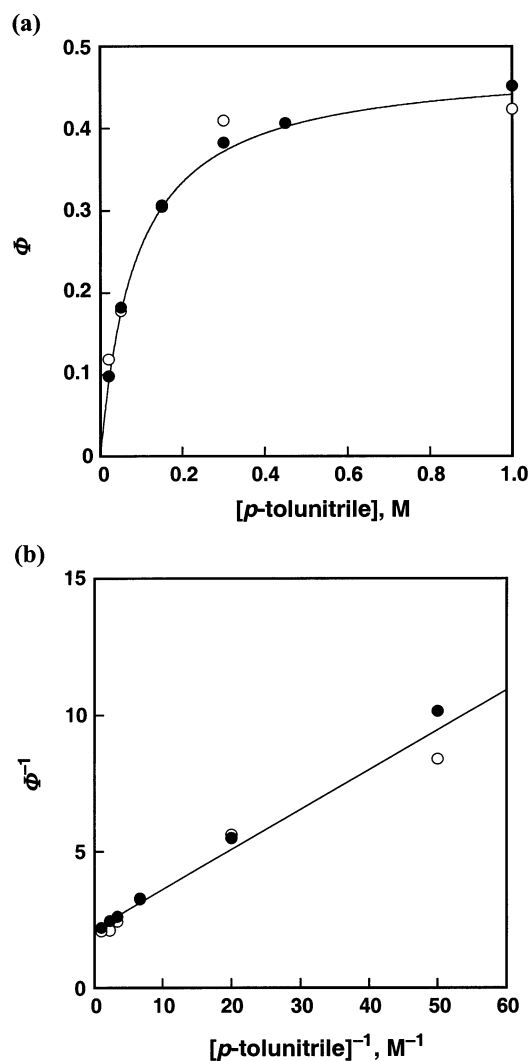


Figure 2. (a) Dependence of the quantum yield (Φ) of *p*-cyanobenzaldehyde for the tetrafluoro-*p*-dicyanobenzene-catalyzed (1.1×10^{-4} M) photooxygenation of *p*-tolunitrile in oxygen- (●) and air- (○) saturated MeCN at 298 K. (b) Plots of Φ^{-1} vs $[p\text{-tolunitrile}]^{-1}$.

rate. The oxygenation of a ring-substituted toluene with an electron-donating substituent, *p*-xylene, by molecular oxygen is also achieved by use of 10-methylacridinium perchlorate ($\text{AcrH}^+\text{ClO}_4^-$) as a photocatalyst. Visible light irradiation of the absorption band ($\lambda_{\text{max}} = 358$ and 417 nm) of AcrH^+ (10 mM) in oxygen-saturated acetonitrile containing *p*-xylene (30

Scheme 1

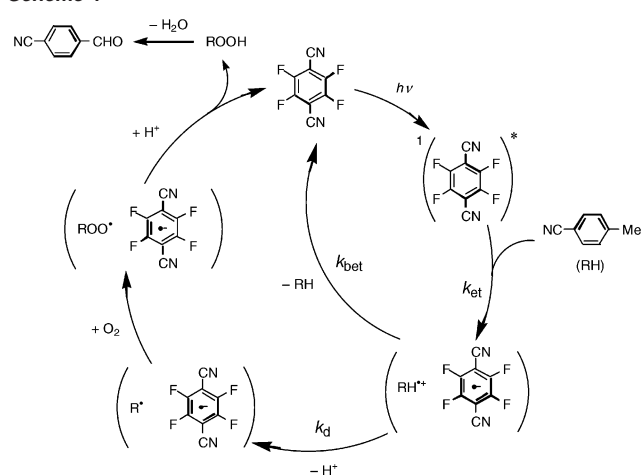
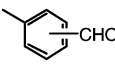
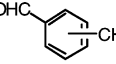
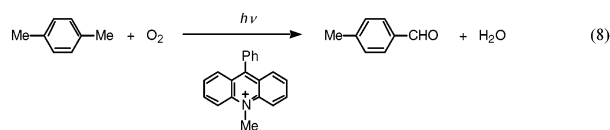


Table 3. Photooxygenation Yields of Xylenes and Toluene (3.0×10^{-2} M), Catalyzed by AcrPh⁺ (1.0×10^{-2} M) with O₂ in O₂-Saturated Chloroform at 298 K^a

	conversion	yield	
		 -CHO	 -CHO
<i>p</i> -xylene	100 %	100 %	0 %
<i>m</i> -xylene	67 %	99 %	1 %
<i>o</i> -xylene	70 %	94 %	6 %
toluene	3 % ^b	100 % ^b	
<i>p</i> -tolualdehyde	0 %		0 %

^a Irradiation time is 10 h. ^b Benzaldehyde.

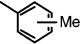
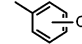
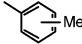
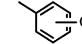
mM) with a xenon lamp through a UV cutoff filter ($\lambda < 310$ nm) results in formation of *p*-tolualdehyde accompanied by disappearance of *p*-xylene. The product was identified by the ¹H NMR spectrum (see Experimental Section). After 24 h of irradiation, the yield of *p*-tolualdehyde was 37%. The product yield is improved to 66% when acetonitrile is replaced by a less polar solvent, chloroform, under otherwise the same experimental conditions. The photooxygenated product yield is further improved to 100% when AcrH⁺ is replaced by AcrPh⁺ in chloroform (eq 8) as shown in Table 3. There were no



dioxygenated products such as *p*-phthalaldehyde and *p*-toluic acid after prolonged photoirradiation. It was confirmed that there was no adduct formation between the photocatalyst, AcrPh⁺, and *p*-xylene. Thus, the 100% selective photooxygenation of *p*-xylene to *p*-tolualdehyde has been accomplished by use of AcrPh⁺ as a photocatalyst in chloroform. The photoirradiation time to obtain 100% yield of *p*-tolualdehyde (3.0×10^{-2} M) was reduced from 24 to 10 h when a xenon lamp was replaced by a high-pressure mercury lamp (1000 W) through an acetophenone–methanol filter ($\lambda < 300$ nm).

Other isomers, *o*- and *m*-xylene, are also converted to *o*- and *m*-tolualdehyde, respectively (Table 4). The product yields of

Table 4. Fluorescence Quenching Rate Constants of AcrH⁺ and AcrPh⁺ by Ring-Substituted Toluenes and Aldehydes in Deaerated MeCN at 298 K

	$k_q, \text{M}^{-1} \text{s}^{-1}$			
	AcrH ⁺		AcrPh ⁺	
	 -Me	 -CHO	 -Me	 -CHO
<i>p</i> -xylene	8.6×10^9	$< 10^6$	1.4×10^{10}	$< 10^8$
	$(4.2 \times 10^9)^a$		$(6.9 \times 10^9)^a$	
<i>m</i> -xylene	7.7×10^9	5.2×10^7	4.7×10^9	$< 10^8$
<i>o</i> -xylene	7.9×10^9	3.8×10^8	6.5×10^9	$< 10^8$
toluene	2.4×10^8	$< 10^{6b}$	$< 10^8$	$< 10^{8b}$

^a Values in parentheses were determined in CHCl₃. ^b Benzaldehyde.

o-, *m*-, and *p*-tolualdehyde and benzaldehyde after 10 h of photoirradiation of an oxygen-saturated chloroform solution of xylenes and toluene (3.0×10^{-2} M) containing AcrPh⁺ (1.0×10^{-2} M) with a mercury lamp ($\lambda < 300$ nm) decreases in the order *p*-xylene > *o*-, *m*-xylene > toluene. The selectivity for tolualdehyde decreases in the order *p*- (100%) > *m*- (99%) > *o*-xylene (94%). The further oxygenation of *m*- and *o*-xylene occurs to yield small amounts of the corresponding phthalaldehyde.

Detection of Reaction Intermediates. The occurrence of photoinduced electron transfer from *p*-xylene to ¹AcrPh⁺ is confirmed by laser flash photolysis experiments (see Experimental Section). Laser excitation ($\lambda = 355$ nm from a Nd:YAG laser) of AcrPh⁺ (1.0×10^{-4} M) in deaerated acetonitrile solution containing *p*-xylene (1.0×10^{-1} M) affords a transient absorption spectrum at 1 μ s with appearance of new absorption bands at 330, 430, 520, and 700 nm with bleaching of AcrPh⁺ at 360 and 420 nm as shown in Figure 3a. Similar transient absorption spectra are also observed in CHCl₃ (see Supporting Information, Figure S2). The transient absorption band at $\lambda_{\text{max}} = 520$ nm is assigned to AcrPh^{*}, since the absorption spectrum of AcrPh^{*} produced independently by the electron-transfer reduction of AcrPh⁺ by tetramethylsemiquinone radical anion (Figure 3b) agrees with the transient absorption spectrum (Figure 3a). The absorption band at 330 nm is assigned to *p*-xylenyl radical, which may be produced by deprotonation of *p*-xylene radical cation.^{44,45} The broad absorption band at $\lambda_{\text{max}} = 700$ nm may be assigned to *p*-xylene dimer radical cation, since similar broad transient absorption bands at a long-wavelength region have been reported for the radical cations of toluene and other aromatic compounds.^{46–49}

- (44) Izumida, T.; Ichikawa, T.; Yoshida, H. *J. Phys. Chem.* **1980**, *84*, 60.
 (45) (a) Sehested, K.; Holcman, J. *J. Phys. Chem.* **1978**, *82*, 651. (b) Hatanaka, K.; Itoh, T.; Asahi, T.; Ichinose, N.; Kawamishi, S.; Sasuga, T.; Fukumura, H.; Masuhara, H. *J. Phys. Chem. A* **1999**, *103*, 11257.
 (46) Liu, A.; Sauer, M. C., Jr.; Loffro, D. M.; Trifunac, A. D. *J. Photochem. Photobiol. A: Chem.* **1992**, *67*, 197.
 (47) (a) Kochi, J. K.; Rathore, R.; Maguères, P. L. *J. Org. Chem.* **2000**, *65*, 6826. (b) Yokoi, H.; Hattai, A.; Ishiguro, K.; Sawaki, Y. *J. Am. Chem. Soc.* **1998**, *120*, 12728.
 (48) (a) Bally, T.; Roth, K.; Straub, R. *J. Am. Chem. Soc.* **1988**, *110*, 1639. (b) Badger, B.; Brocklehurst, B. *Trans. Faraday Soc.* **1969**, *65*, 2582 and 2588. (c) Gerson, F.; Kaupp, G.; Ohya-Nishiguchi, O. *Angew. Chem., Int. Ed. Engl.* **1977**, *16*, 657. (d) Badger, B.; Brocklehurst, B. *Trans. Faraday Soc.* **1970**, *66*, 2939. (e) Rodgers, M. A. J. *J. Chem. Soc., Faraday Trans.* **1972**, *68*, 1278. (f) Inokuchi, Y.; Naitoh, Y.; Ohashi, K.; Saitow, K.-I.; Yoshihara, K.; Nishi, N. *Chem. Phys. Lett.* **1997**, *269*, 298.
 (49) For dimer radical anions of electron acceptors, see Ganesan, V.; Rosokha, S. V.; Kochi, J. K. *J. Am. Chem. Soc.* **2003**, *125*, 2559.

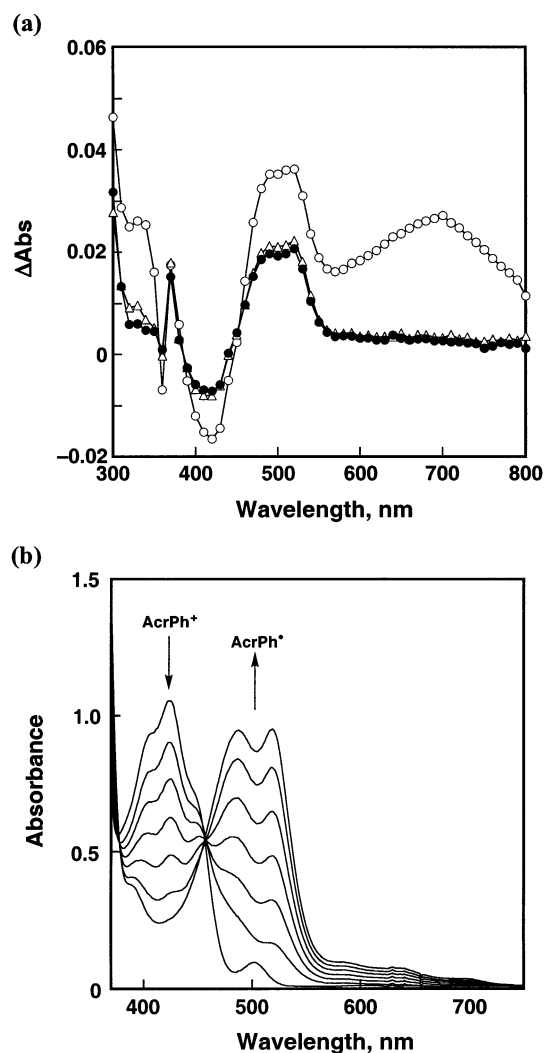


Figure 3. (a) Transient absorption spectra observed by photoexcitation of the argon- (○), air- (△), and oxygen- (●) saturated MeCN solution of AcrPh⁺ (1.0×10^{-4} M) and *p*-xylene (1.0×10^{-1} M) at 1 μs after laser excitation at 298 K. (b) Spectral change upon addition of Me₄Q^{•-} (0, 2.8×10^{-5} , 5.6×10^{-5} , 8.4×10^{-5} , 1.1×10^{-4} , 1.4×10^{-4} , and 1.7×10^{-4} M) to a deaerated MeCN solution of AcrPh⁺ (1.7×10^{-4} M) at 298 K.

To confirm the generation of *p*-xylene dimer radical cation, dependence of ΔAbs at 700 nm on the concentration of *p*-xylene was examined in CHCl₃ as shown in Figure 4a, where ΔAbs at 700 nm increases with an increase in the concentration of *p*-xylene to approach a limiting value. Such a saturated dependence of ΔAbs on concentration of *p*-xylene indicates the existence of an equilibrium between the monomer and the dimer radical cation. The formation constant of the dimer radical cation is determined as 1.4×10^2 M⁻¹ from the slope and the intercept of a linear plot of ΔAbs⁻¹ vs [*p*-xylene]⁻¹ (Figure 4b).

The absorption bands at 520 nm due to AcrPh* decays obeying second-order kinetics. The second-order plot of [AcrPh*] obtained from the absorbance at 520 nm with the ε value of 3.9×10^3 M⁻¹ cm⁻¹ can be fit to a line (Supporting Information, Figure S3). The ε value of AcrPh* in CHCl₃ is determined from the titration of AcrPh⁺ with tetramethylsemiquinone radical anion (Figure S3). The second-order decay rate constant is determined from the slope as 1.1×10^{10} M⁻¹ s⁻¹, which is nearly the same as the diffusion-limited value in CHCl₃ (1.2×10^{10} M⁻¹ s⁻¹).³⁸

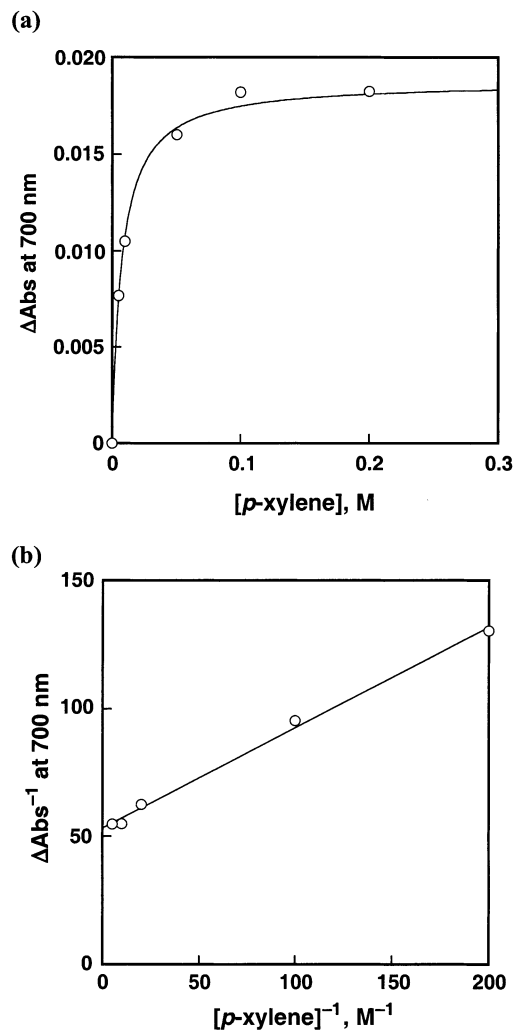


Figure 4. (a) Plots of ΔAbs at 700 nm vs [*p*-xylene] in the photoinduced electron transfer from *p*-xylene to AcrPh⁺ in deaerated CHCl₃ at 1.0 μs after laser excitation at 298 K. (b) Plots of ΔAbs⁻¹ vs [*p*-xylene]⁻¹.

When oxygen is introduced to the AcrPh⁺–*p*-xylene system in acetonitrile, the broad absorption band at 700 nm due to *p*-xylene dimer radical cation disappears as shown in Figure 3a (air- and oxygen-saturated solution), whereas the absorption band due to AcrPh* at 520 nm remains. This indicates that oxygen reacts with *p*-xylenyl radical produced by deprotonation of *p*-xylene radical cation, which is in equilibrium with the dimer radical cation, rather than with AcrPh*. The deprotonation of radical cations of toluene and *p*-xylene is known to occur efficiently.^{45,50} In the presence of oxygen, *p*-xylenyl radical reacts with oxygen in competition with the back electron transfer from AcrPh* to *p*-xylene radical cation to give the peroxy radical, which was detected successfully by ESR (vide infra).

An oxygen-saturated dichloromethane solution of *p*-xylene (5.0×10^{-1} M) with AcrPh⁺ (1.0×10^{-2} M) was irradiated by a high-pressure mercury lamp at 203 K. The resulting ESR spectrum consists of two isotropic signals at $g = 2.0151$ and at $g = 2.0034$ (Figure 5a). The former signal is readily assigned to *p*-xylenylperoxy radical because the g value is diagnostic of peroxy radicals.⁵¹ The latter signal is assigned to AcrPh*,

(50) (a) Masnovi, J. M.; Kochi, J. K. *J. Am. Chem. Soc.* **1985**, *107*, 6781. (b) Masnovi, J. M.; Kochi, J. K. *J. Phys. Chem.* **1987**, *91*, 1878. (c) Maguères, P. L.; Lindeman, S. V.; Kochi, J. K. *J. Chem. Soc., Perkin Trans. 2*, **2001**, 1180.

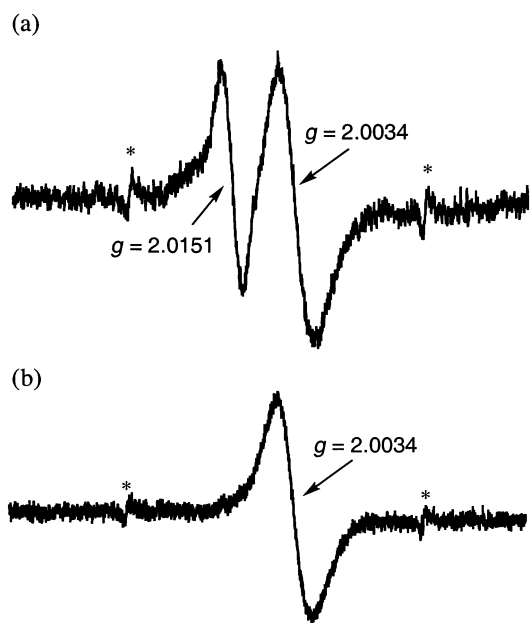
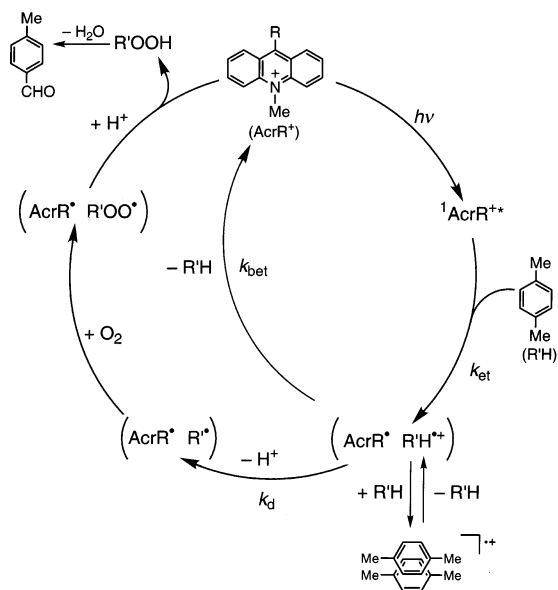


Figure 5. ESR spectra observed under photoirradiation of (a) oxygen- and (b) argon-saturated CH_2Cl_2 solution of AcrPh^+ (1.0×10^{-2} M) containing *p*-xylene (5.0×10^{-1} M) at 203 K. The asterisk denotes an Mn^{2+} ESR marker.

Scheme 2



on the basis of the agreement between the reported and observed g value.²³ In the absence of oxygen, only the latter signal is observed under otherwise identical experimental conditions (Figure 5b).⁵²

Photocatalytic Oxygenation Mechanism. Based on the above results, the reaction mechanism for the AcrR^+ -photosensitized oxygenation ($\text{R} = \text{H}$ and Ph) of *p*-xylene is given as shown in Scheme 2. Photoinduced electron transfer from *p*-xylene to $^1\text{AcrR}^{+\ast}$ (k_{et}) occurs to produce AcrR^* and *p*-xylene radical cation, which is in equilibrium with the dimer radical

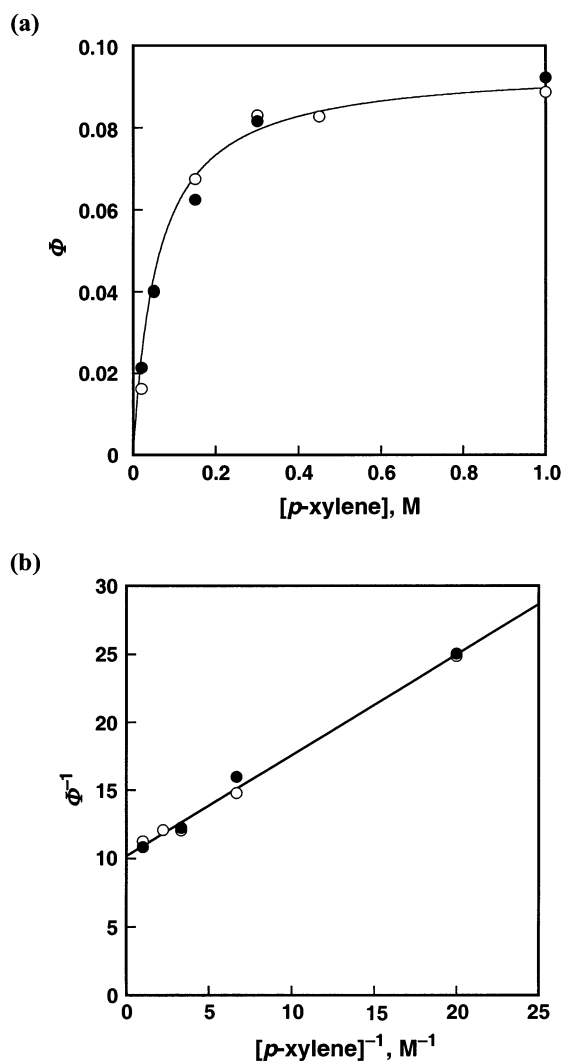


Figure 6. (a) Dependence of the quantum yield (Φ) of *p*-tolualdehyde for the AcrPh^+ -catalyzed (1.1×10^{-4} M) photooxygenation of *p*-xylene in air- (○) and oxygen- (●) saturated CHCl_3 at 298 K. (b) Plots of Φ^{-1} vs $[\textit{p}\text{-xylene}]^{-1}$.

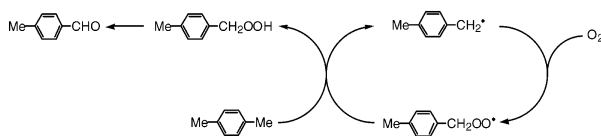
cation as seen in Figure 3a. This is followed by deprotonation of *p*-xylene radical cation to give *p*-xylene radical in competition with the back electron transfer (k_{bet}) to the reactant pair. In the presence of oxygen, *p*-xylene radical is readily trapped by oxygen to give *p*-xyleneperoxy radical as observed in Figure 5a. The *p*-xyleneperoxy radical is reduced by back electron transfer from AcrR^* to yield *p*-xylene hydroperoxide, accompanied by regeneration of AcrR^+ (Scheme 2). The hydroperoxide decomposes to yield *p*-tolualdehyde selectively.

According to Scheme 2, the quantum yield (Φ) for the AcrR^+ -catalyzed photooxygenation of *p*-xylene is expressed as a function of concentration of *p*-xylene as in the case of the photocatalytic oxygenation of *p*-tolunitrile (eq 7). The Φ values of the AcrPh^+ -catalyzed photooxygenation of *p*-xylene with O_2 in air- and oxygen-saturated CHCl_3 were determined from the product formation rate under irradiation of monochromatized light of $\lambda = 358$ nm (see Experimental Section). The Φ values were the same at different oxygen concentrations (Figure 6a). The Φ value increases with an increase in concentration of *p*-xylene to approach a limiting value (Φ_{∞}) in accordance with eq 7 (Figure 6a). The linear plot of Φ^{-1} and $[\textit{p}\text{-xylene}]^{-1}$ in accordance with eq 8 as shown in Figure 6b. From the slope

(51) Cumylperoxy radical has been reported as $g = 2.0156$: (a) Bersohn, M.; Thomas, J. R. *J. Am. Chem. Soc.* **1964**, *86*, 959. (b) Fukuzumi, S.; Ono, Y. *J. Chem. Soc., Perkin Trans. 2* **1977**, 622.

(52) The ESR signal due to *p*-xylene dimer radical cation may be overlapped with that of AcrPh^* .

Scheme 3



and intercept in Figure 6b, the Φ_∞ and K_{obs} values are obtained as 0.10 and 14 M^{-1} , respectively. The K_{obs} value can be converted to the corresponding rate constant (k_{obs}) provided that the excited state of AcrPh^+ involved in the photocatalytic reaction is a singlet ($k_{\text{obs}} = K_{\text{obs}}\tau^{-1}$, $\tau = 2.2 \text{ ns}$ for $^1\text{AcrPh}^{+*}$). The k_{obs} value thus obtained ($6.3 \times 10^9 \text{ M}^{-1} \text{ s}^{-1}$) agrees well with the corresponding k_{et} value ($6.9 \times 10^9 \text{ M}^{-1} \text{ s}^{-1}$) determined independently by fluorescence quenching. Such agreement strongly supports the reaction mechanism in Scheme 2 where the photocatalytic reaction is initiated by photoinduced electron transfer from *p*-xylene to $^1\text{AcrR}^{+*}$.

The thermal oxygenation reaction of *p*-xylene with oxygen is proposed to proceed via radical chain processes as shown in Scheme 3.^{53–55} The *p*-xylene radical cation is assumed to be produced by direct electron transfer from *p*-xylene to oxygen in a charge-transfer complex between them.⁵⁴ However, the saturated dependence of Φ on $[\text{D}]$ in Figure 6a indicates that such an electron-transfer radical chain process (Scheme 3) is not operative as the major pathway in the present photocatalytic reaction.

If the chain process in Scheme 3 were the major pathway, the Φ value would increase linearly with increasing concentration of *p*-xylene.

No photooxygenation of 2,5-dimethoxytoluene, the strongest electron donor in this study, has occurred with AcrPh^+ as a photocatalyst in CHCl_3 , probably because of the slow deprotonation rate as compared with the fast back electron transfer despite the efficient fluorescence quenching of AcrPh^+ by 2,5-dimethoxytoluene ($k_{\text{q}} = 1.2 \times 10^{10} \text{ M}^{-1} \text{ s}^{-1}$).

The 100% selective photocatalytic oxygenation of *p*-xylene is made possible by the difference in the reactivity of *p*-xylene and the oxygenated product, *p*-tolualdehyde, as indicated by the following fluorescence quenching experiments. The fluorescence lifetimes (τ) of AcrH^+ ($\lambda_{\text{em}} = 488 \text{ nm}$) in the absence and presence of xylenes, toluene, or the corresponding aldehydes were determined with the time-resolved fluorescence spectrofluorophotometer. The rate constants of fluorescence quenching k_{q} ($= K_{\text{q}}\tau^{-1}$) by photoinduced electron transfer are determined from the slopes of the linear Stern–Volmer plots of τ_0/τ ($\tau_0 = 37 \text{ ns}$ in MeCN)²³ vs the quencher concentration. The k_{q} values thus determined are listed in Table 4 (see typical data in Supporting Information, Figure S4).

The $^1\text{AcrH}^{+*}$ fluorescence was quenched efficiently by electron transfer from xylenes to $^1\text{AcrH}^{+*}$, whereas no quenching was observed by *p*-tolualdehyde ($k_{\text{q}} \ll 1 \times 10^7 \text{ M}^{-1} \text{ s}^{-1}$). The k_{q} value decreases in the order *p*-xylene > *o*-xylene > *m*-xylene > *o*-tolualdehyde > toluene > *m*-tolualdehyde \gg *p*-tolualdehyde (not observed). This order is consistent with the order of the monoxygenated and dioxygenated product yields

in Table 4. Thus, the faster the photoinduced electron transfer, the larger the product yield. However, the k_{q} value for *p*-xylene determined in chloroform ($4.2 \times 10^9 \text{ M}^{-1} \text{ s}^{-1}$) is smaller than the value in acetonitrile in Table 4, in contrast to the improved product yield in chloroform as compared to that in the more polar solvent acetonitrile (vide supra).

The improved product yield in chloroform may result from a decrease in the reorganization energy for the electron transfer with decreasing the solvent polarity, which results in the slower back electron transfer from AcrH^+ to *p*-xylene radical cation in Scheme 2 (vide infra).²³ Since the deprotonation of *p*-xylene radical cation, which leads to the oxygenated product, competes with the back electron transfer, the slower back electron transfer results in the larger product yield.

The smaller reorganization energy in CHCl_3 (0.27 eV) than in acetonitrile (0.34 eV) has been confirmed by determining the rate constants of electron-transfer self-exchange reactions between 10-methyl-9-phenylacridinium ion (AcrPh^+) and the corresponding one-electron-reduced radical (AcrPh^*) in acetonitrile and chloroform.²³ Since the λ values (0.27, 0.34 eV) are much smaller than the driving force of the back electron transfer ($-\Delta G_{\text{et}}^0 = 2.36 \text{ eV}$) from AcrH^+ (E_{ox}^0 vs SCE = -0.43 V)²⁹ to *p*-xylene radical cation ($E_{\text{red}}^0 = 1.93 \text{ V}$),²³ the back electron transfer is deeply in the Marcus inverted region, where the back electron-transfer rate is expected to slow with decreasing λ value.^{23,24} The slower back electron-transfer rate with decreasing solvent polarity leads to an increase in the product yield as observed experimentally (see Supporting Information, Figure S5).

Further improvement of the product yield by employing AcrPh^+ instead of AcrH^+ can also be ascribed to the slower back electron-transfer rate for the former than the latter. Since the E_{ox}^0 value of AcrPh^+ (E_{ox}^0 vs SCE = -0.55 V)²³ is more negative than the value of AcrH^+ (E_{ox}^0 vs SCE = -0.43 V),²⁹ the driving force of the back electron transfer from AcrPh^+ (2.48 eV) is larger than that from AcrH^+ (2.36 eV). The larger driving force thereby results in slower back electron transfer, leading to improved product yield.

The enhanced stability of AcrPh^+ as a photocatalyst as compared to AcrH^+ is ascribed to the steric effect of the phenyl group of AcrPh^+ , which hampers the radical coupling with deprotonated radicals that could be the deactivation process of the photocatalyst in Scheme 2.

In conclusion, the use of AcrPh^+ as a photocatalyst in chloroform has enabled us to accomplish the 100% selective photooxygenation of *p*-xylene to *p*-tolualdehyde as well as highly selective photooxygenation of other isomers to the corresponding aromatic aldehydes. Photooxygenation of a ring-substituted toluene with an electron-withdrawing substituent (*p*-tolunitrile) by molecular oxygen is also made possible by use of tetrafluoro-*p*-dicyanobenzene as the photocatalyst for the photooxygenation of *p*-tolunitrile. Thus, selective photooxygenations of ring-substituted toluenes are finely controlled by choosing an appropriate photocatalyst with different one-electron redox potentials and solvents.

Acknowledgment. This work was partially supported by a Grant-in-Aid for Scientific Research Priority Area (11228205) from the Ministry of Education, Culture, Sports, Science and Technology, Japan.

(53) Nelsen, S. F.; Kapp, D. L.; Akaba, R.; Evans, D. H. *J. Am. Chem. Soc.* **1986**, *108*, 6863.

(54) Correa, P. E.; Hardy, G.; Riley, D. P. *J. Org. Chem.* **1988**, *53*, 1695.

(55) Clennan, E. L.; Simmons, W.; Almgren, C. W. *J. Am. Chem. Soc.* **1981**, *103*, 2098.

Supporting Information Available: Five figures showing Stern–Volmer plot for the fluorescence quenching of various photosensitizers by *p*-tolunitrile, transient absorption spectra of the photoinduced electron transfer from *p*-xylene to $^1\text{AcrPh}^{+\bullet}$ in CHCl_3 , decay time profile of AcrPh^\bullet , Stern–Volmer plots

for the fluorescence quenching of AcrPh^+ by ring-substituted toluenes, and irradiation time dependence of the yield of *p*-tolualdehyde (PDF). This material is available free of charge via the Internet at <http://pubs.acs.org>.

JA036645R